2024 IEEE/RSJ International Conference on Intelligent Robots and Systems (IROS)
October 14-18, 2024. Abu Dhabi, UAE

Peristaltic Soft Robot for Long-distance Pipe Inspection with an Endoskeletal Structure for Propulsion and Traction Amplification

R. Okuma, Y. Naruse, *Member, IEEE*,
F. Ito, *Graduate student member, IEEE*, and T. Nakamura, *Member, IEEE*

***Abstract*— This study proposed a peristaltic motion-type inspection robot equipped with a "linear antagonistic mechanism using artificial muscles with an endoskeletal structure" to amplify propulsion and traction. We sought to develop an in-pipe inspection robot for long, narrow, and complex pipes requiring large propulsion, traction, and flexibility. In a previous study, we proposed a linear antagonistic mechanism allowing the inspection robot to generate both high propulsion and traction along with flexibility in narrow pipes. The proposed mechanism consisted of two extension actuators and a gripping actuator sandwiched between these extension actuators. The large extension force by the extension actuators is distributed to both propulsion and traction. However, owing to the piston-shaped configuration of the extension actuators, the generated force decreased in a manner dependent on the cross-sectional area within narrow pipelines. Therefore, the in-pipe inspection robot took time to move in long-distance, small-diameter pipes with multiple bends. This paper describes a "linear antagonistic mechanism using artificial muscles with an endoskeletal structure" that amplifies propulsion and traction by inserting a tension spring (skeleton) inside the contraction actuators (artificial muscles) and utilizing the action force generated by the actuator and transmitted by the tension spring. In this study, the developed robot with an endoskeleton exhibited maximum propulsion of 60.2 N, surpassing its non-endoskeleton counterpart by a factor of 1.61. Furthermore, the robot equipped with the endoskeleton passed through an elbow pipe 1.29 times faster than that without the endoskeleton, reducing the time from 741 to 576 s. The function value that compares the propulsion and traction considering the effects of the applied pressure and pipe diameter required for long-distance inspection was more than 1.13 times that of the previous study. In addition, the non-dimensionalized traction was 1.55 times greater than that of any other pipe inspection robot, and the propulsion was large enough to pass through a bending pipe. This result indicates the feasibility of the developed robot for inspecting long, narrow, and complex pipes.**

I. Introduction

Pipelines installed in various industrial facilities and residential areas are vital infrastructure components. The long-term use of these pipes can result in corrosion and cracking within the pipes, resulting in reduced transport efficiency and liquefaction. Addressing this concern necessitates the regular internal inspection of pipelines [1]. However, traditional manual inspection methods by human personnel pose substantial challenges in inspecting and cleaning the interiors of long-distance, small-diameter pipes with multiple bends [2]. Therefore, using in-pipe inspection robots has garnered considerable attention [3-15].

There are several types of in-pipe inspection robots, such as wheel-type [4-7], crawlers [8], snake [9, 10], walking [11, 12], cilia vibration [13], and wave propagation [14, 15]. Many wheel-type, crawler-type, and snake-type in-pipe inspection robots have complex structures and large mechanisms. Therefore, adapting them to move and inspect complex narrow pipes is challenging [16-18]. The walking-type robots have a limited contact area with the pipe wall, making it difficult for them to transverse long-distance pipes because of the lack of traction. The cilia vibration-type robot is easy to miniaturize and has a flexible structure. However, applying these robots to vertical and backward movements is difficult. In contrast, hydrodynamic-driven wave-propagation-type in-pipe inspection robots are compact, capable of generating significant force, and possess a flexible structure. Hence, they are expected to be applied to the inspection and cleaning of long-distance, small-diameter, complex pipes. However, these robots face several challenges. The fluid pressure generates force only in the direction perpendicular to its cross-section. Therefore, conventional robots use the cross-sectional area of a small pipe to generate the large extendable force, and the passive force generated by the material that makes up the fluid-pressure-type extendable actuators and fluid-pressure force are antagonized. However, this method fails to enhance the force generated in the contraction and extension directions of the robot unless the elastic force of the actuator is augmented. Moreover, the stiffness of the actuator increases in the circumferential direction of the pipe during extension or retraction. Therefore, when both the propulsion and traction are increased, the rigidity of the robot increases, impeding its ability to navigate complex pipes.

This study aimed to develop an in-pipe inspection robot mechanism capable of enhancing propulsion and traction using large force generated by hydrodynamic actuators. The force generated by the fluid pressure was determined by multiplying the cross-sectional area with the pressure. Given the elongated and narrow nature of the target pipe, there was a limited cross-sectional area for generating force. Placing the actuators in parallel within such a pipe did not increase the generated force. To address this challenge considering the principle of fluid pressure force, a system is required to convert the active generating force of series-connected actuators in a long, narrow pipe into propulsion and traction for the robot. Therefore, we proposed a linear antagonistic mechanism that comprises a gripping actuator that fixes the robot between two

All authors are with the Faculty of Science and Engineering, Chuo University, 1-13-27 Kasuga, Bunkyo-ku, 112-8551 Tokyo, Japan. (Corresponding author e-mail: a19.mmw3@g.chuo-u.ac.jp).

979-8-3503-7769-9/24/$31.00 ©2024 IEEE

hollow extendable actuators. The distance between the two end faces of the two extendable actuators was constrained such that it did not change. When one of the extendable actuators was extended while the central gripping actuator was fixed to the pipe, the other extendable actuator was forced to contract. Thus, the mechanism can exert both propulsion and traction through the active generation of extendable actuators.

In a previous study [19], we developed a wave-propagation-type in-pipe inspection robot, PI-RO, with a linear antagonistic mechanism. This robot uses pneumatic piston-shaped flexible extendable actuators interconnected through wires to augment its traction capabilities. The PI-RO outperformed other systems with a 2.57 times higher non-dimensionalized evaluation function for the sum of propulsion and traction, considering the differences in applied pressure and inner pipe diameter. Furthermore, the PI-RO was moved into a pipe with an inner diameter of 28 mm, a length of 11.7 m, and a bend. These results demonstrate that an in-pipe inspection robot equipped with a linear antagonistic mechanism can move and inspect long, narrow, and complex pipes. However, the piston-shaped actuators used in the previous study decreased the force generated depending on the cross-sectional area of the pipe. Consequently, the speed of the robot was affected, resulting in occasional stops in long, narrow, and complex pipelines. Additionally, the passive restoration of the unit led to low propulsion, while the traction was affected by the load during locomotion to prevent full expansion of the grip unit. As a result, the robot exhibited low propulsion and traction. Therefore, it is necessary to develop a mechanism capable of exerting both propulsion and traction, facilitated by actuators capable of generating large force even within elongated pipes.

This study proposed a linear antagonistic mechanism using artificial muscles with an endoskeletal structure by inserting a tension spring (skeleton) inside contraction actuators (artificial muscles) to increase propulsion and traction while maintaining high flexibility (Fig. 1) [20]. In contrast to a typical piston-shaped hydrodynamic actuator, a contraction actuator converts the fluid pressure received by the circumferential surface into the axial contraction force. Therefore, the cross-sectional area receiving fluid pressure within a narrow pipe can be increased, and relatively large force can be generated, even in long, narrow pipes. In addition, the actuator is flexible and can assist in passage through bent pipes. Hence, we hypothesized that more propulsion and traction could be exerted by serially antagonizing the artificial muscles than with the piston-shaped actuators. The proposed mechanism is sufficiently flexible to pass through bent pipes and convert the contraction force of antagonized extendable actuators into propulsion and traction. Therefore, the restraint placed at the endpoints of the extendable actuator encounters difficulties in axial contraction relative to the travel direction and must be bent in the Yaw and Pitch directions in the bending pipe. Moreover, the restraint must be incorporated into the robot without interfering with endoscope wirings. Therefore, a tensile spring was selected. The tension springs are circular, bendable, and difficult to contract in the axial direction. In addition, this spring design allows seamless endoscope passage, mitigating potential interference with the endoscope wiring and restraining elements. The performance of the robot developed in the

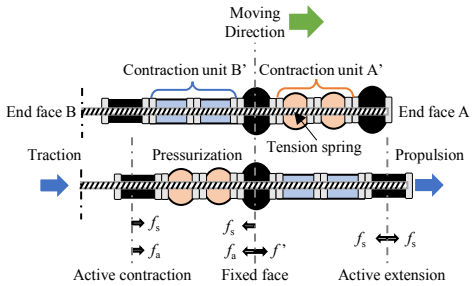

Fig. 1. Schematic of the linear antagonistic mechanism using artificial muscles with an endoskeletal structure.

Table. 1. List of symbols and nomenclatures of the linear antagonistic mechanisms using artificial muscles with an endoskeletal structure.

Symbol	Definition	Unit
f_a	Active contraction force of the contraction unit.	N
f_s	Passive extension force of the contraction unit.	N
f'	Force generated in the axial direction of the fixed end.	N
f_{Pro}	Propulsion force by mechanism.	N
f_{Tra}	Traction force by mechanism.	N

previous study was showcased through experiments measuring its movement speed within a straight pipe. However, neither the traction nor propulsion of the robot has been quantified. Consequently, the design and development of the proposed robot pose challenges in considering the morphology of the target pipeline.

This paper describes a flexible endoskeletal mechanism of the earthworm-type robot enhancing both the propulsion and traction to inspect long, narrow, and complex pipelines. Force is necessary to inspect long distances or complex pipes. If the propulsion is low, the speed decreases when a load acts on the movement of the robot. If the traction is low, the frictional force on the wiring in long, complex pipes becomes large, impeding the robot's movement. In this study, an endoskeletal structure was implemented into a peristaltic motion-type inspection robot capable of crawling in narrow and complex spaces with high traction, and experimental results were compared to determine whether it could efficiently output propulsion and traction.

Section II describes the concept and design method of the robot. In Section III, the overall configuration and components of the developed robot are presented. In Section IV, we discuss propulsion and traction measurement experiments using the developed robot. In Section V, the results of the elbow pipe passage experiment are presented. Section VI discusses the results of a comparison of propulsion, traction, and flexibility of the developed robot based on the evaluation function. Finally, Section VII presents the summary and directions for future work. The contributions of this study are as follows:

- A linear antagonistic mechanism using artificial muscles with an endoskeletal structure was proposed to enhance propulsion and traction.
- The developed robot exhibited a maximum propulsion of 60.3 N, which was 1.61 times greater than that without the proposed mechanism. Additionally, it demonstrated a high traction of 538.9 N.
- The value of the evaluation function was 1.13 times higher than that of the robot in the previous study when the

effects of the applied pressure and inner diameter of the pipe were considered.

- The developed robot passed through the elbow pipe 1.29 times faster than the robot without the proposed mechanism.

II. Design

This section describes the concept, design method, theoretical model of propulsion and traction, and the unit design of a linear antagonistic mechanism using artificial muscles with an endoskeletal structure.

A. Requirement Specification

The method proposed in this study allows the contraction force produced by multiple actuators arranged in series to be used as the extension force of other actuators, thereby influencing their motion. This instance of the element of one muscle contraction force generating extension force in another muscle is also observed in biology. For instance, earthworms independently control multiple body segments to generate force in the direction of muscle extension via muscle contraction. Therefore, the development of a method to convert the muscle contraction force into the extension force may enable the application of these biological advantages in robotics. Furthermore, reproducing these principles using a robotic mechanism may pave the way for the creation of robots that exploit novel locomotion features not yet observed in earthworms.

This study presents the feasibility of the proposed mechanism as a first step in this research. We focused on inspecting inverted pipes with diameters of about 54 mm, denoted as 50A, to demonstrate the effectiveness of the robot in pipe inspection. The commonly inspected pipe is a standard 15 m long steel pipe with an inner diameter of approximately 55 mm. The piping has multiple 90-degree bends, which create height differences in the piping path. Considering the current use of piping, the entire pipeline must be inspected within one hour. Based on the aforementioned parameters, the requirements for an in-pipe inspection robot are summarized as follows:

- Inspecting a round trip of 30 m within the pipes
- Inspecting pipes with an inner diameter of 55 mm
- Inspecting complex, long-distance pipes featuring elevation differences with multiple elbow pipes
- Inspecting entire pipes in less than one hour

B. Linear Antagonistic Mechanism by Endoskeletal Type Artificial Muscles

The operation of a linear antagonistic mechanism using endoskeletal artificial muscles is shown in Fig. 1. The mechanism consisted of two contraction units A' and B', and a tension spring. In addition, the linkage parts of each unit were actively fixed and released. When the central grip unit was fixed at the center, the contraction unit A' was extended, and simultaneously, the contraction unit B' was contracted to generate active pushing force on end-face A. In addition, the pushing force was transmitted by the tension spring connected to end-face A. Fig. 1 shows the propulsion f_{Pro} acting on end-face A and the traction f_{Tra} acting on end-face B generated by the mechanism expressed in (1) and (2), respectively, using the definitions listed in Table. 1.

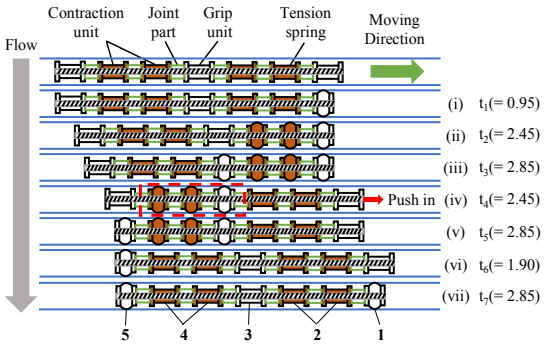

Fig. 2. Operation pattern of the robot to be developed.

$$f_{\mathrm{Pro}} = f_{\mathrm{s}} \tag{1}$$

$$f_{\mathrm{Tra}} = f_{\mathrm{a}} + f_{\mathrm{s}} \tag{2}$$

C. Configuration and Movement Patterns of the Developed Robot Mechanism

Fig. 2 shows the operational configuration of the robot to be developed. The robot consists of three grip units and two contraction units. The contraction units of this mechanism are applied to a configuration connected to two grip units. We hypothesized that a contraction unit with a structure separate from the grip unit would have lower scalability, maintainability, and fault tolerance. Therefore, the same basic structure of the mechanism as that of the grip unit enables a robust response to failure.

The operation of the developed robot is as follows. (i) The grip unit 1 gripped the pipe. (ii) The contraction unit 2 contracted. (iii) The grip unit 3 gripped the pipe. (iv) The grip unit 1 released the pipe, the contraction unit 2 extended, and simultaneously, the contraction unit 4 contracted, thereby pushing the internal tension spring in the forward direction. The active contraction force of the contraction unit 4 was transmitted by the tension spring to exert propulsion, as expressed in (1) and illustrated on the right side of Fig. 2. (v) The gripping unit 5 gripped the pipe. (vi) The grip unit 3 released the pipe and the contraction unit 4 extended. (vii) The grip unit 1 gripped the pipe. This mechanism caused the robot to move forward in the pipe by repeating movements (i) to (vii).

D. Grip Unit

Fig. 3(a) shows the prototype grip unit. The unit consisted of two flanges, two tightening rings, bellows, and a straight-fiber-type artificial muscle [21] with a thickness of 1 mm, which has a longer lifetime than the McKibben types and exhibits very high durability. Pressurized air flowed between the bellows and artificial muscles into the chamber, causing the unit to grip the pipeline by expanding radially beyond the inner diameter of the pipe. When depressurized, the unit returns to its initial state owing to the elasticity of the constituent materials and stops gripping. The unit has a hollow structure into which air tubes, a tension spring, and an endoscope can be inserted. The unit was surrounded by a nylon brush [15], which reduced the frictional force caused by the grip unit in contact with the inner wall of the pipe. In this study, the artificial muscle of the grip unit was designed to be longer than that of the contraction unit. Consequently, the increased contact between the artificial muscle section and the inner wall of the pipe during pressurization was expected to result in

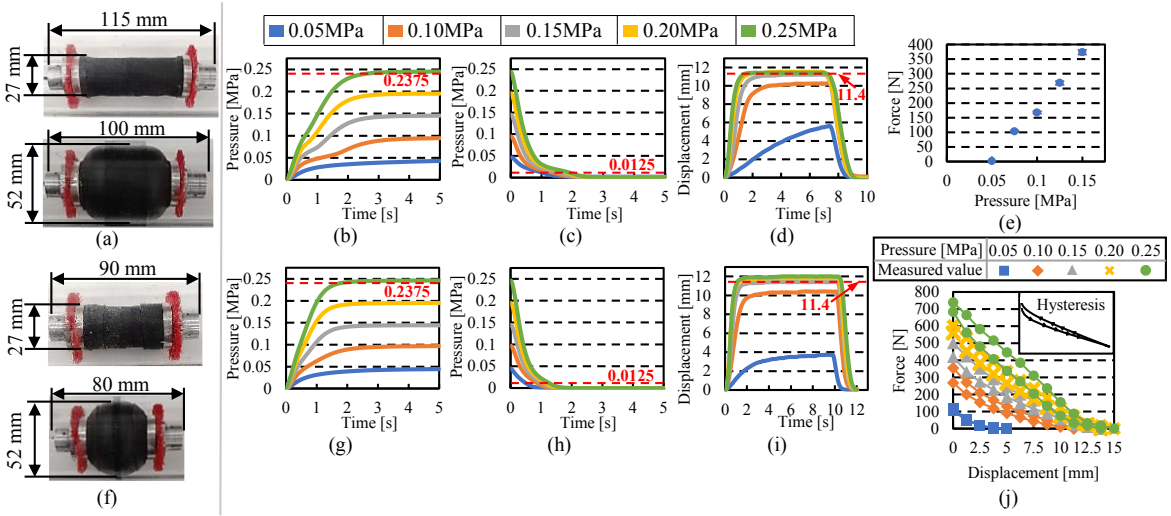

Fig. 3. Appearance and characteristics of the actuators that compose the robot. (a) Grip unit, (b) Air supply response of the grip unit, (c) Exhaust response of the grip unit, (d) Displacement response of the grip unit, (e) Traction of the grip unit, (f) Contraction unit, (g) Air supply response of the contraction unit, (h) Exhaust response of the contraction unit, (i) Displacement response of the contraction unit, (j) Contractile force characteristics of each displacement of the contraction unit.

significant frictional force, enhancing the gripping force.

The air supply, exhaust, and displacement responses of the grip unit are illustrated in Figs. 3(b), 3(c), and 3(d), respectively. In these measurements, air pressure controlled by a proportional solenoid valve was applied to the grip unit through an air tube with an inner diameter of 2 mm and length of 0.2 m, which was connected to an air tube with an inner diameter of 4 mm and length of 10 m via a rapid exhaust valve. When 0.25 MPa was applied, the internal pressure reached 95% of the applied pressure at 2.58 s (Fig. 3(b)) and 5% of the applied pressure at 2.00 s (Fig. 3(c)). In contrast, when 0.25 MPa was applied, as shown in Fig. 3(d), the maximum contraction occurred at 1.90 s. As described above, the internal pressure did not increase even when maximum contraction was reached. Thus, when 0.25 MPa was applied to the grip unit as the upstream pressure for 2.58 s or longer, the internal pressure increased more than 0.95 times while the grip unit gripped the pipe. The maximum contraction of the grip unit was 12 mm, which was almost constant at pressures higher than 0.15 MPa, as shown in Fig.3(d). Fig. 3(e) shows the maximum static friction force on the grip unit. The maximum static friction force increased linearly with internal pressure. The artificial muscle force pressing against the pipe increased with an increase in pressure. The maximum static friction force was 374 N at an applied pressure of 0.15 MPa. When the applied pressure was 0.05 MPa, the grip unit did not expand beyond the inner diameter of the pipe.

E. Contraction Unit

Fig. 3(f) shows the contraction unit. The contraction unit consisted of two connected units. The basic structure is similar to that of the grip unit, thereby enabling high scalability and maintainability. Both units simultaneously contracted axially and expanded radially during pressurization to the extent that they did not grip the inner wall of the pipe. The active contraction force was transmitted by the tension spring while simultaneously pulling the wiring and pushing the robot forward. When depressurized, the unit returned to its initial state because of the elasticity of its constituent materials.

The air supply, exhaust, and displacement responses of the contraction unit are presented in Figs. 3(g), 3(h), and 3(i), respectively. Air pressure was applied using the same method used for the grip unit. When 0.25 MPa was applied, the internal pressure reached 95% of the applied pressure at 1.84 s (Fig. 3(g)) and 5% of the applied pressure at 1.38 s (Fig. 3(h)). In contrast, when 0.25 MPa was applied as shown in Fig. 3(i), maximum contraction occurred at 1.10 s. As in the case of the grip unit, when 0.25 MPa was applied to the contraction unit as the upstream pressure for 1.84 s or longer, the internal pressure increased more than 0.95 times. Fig. 3(j) shows the relationship between the contraction force and contraction length of the artificial muscle for each applied pressure of the contraction unit.

Based on the basic characteristics of these units, the propulsion and traction of the model are expected to be higher than those of conventional robots. This indicates that the proposed mechanism can exert both propulsion and traction, such that the robot can pass through multiple bent pipes. Therefore, a robot equipped with a linear antagonistic mechanism using artificial endoskeleton muscles was developed in this study.

III. Development

This section describes the overall configuration and components of the developed robot.

A. Developed Robot

Fig. 4(a) shows an in-pipe inspection robot equipped with a linear antagonistic mechanism using artificial endoskeletal muscles. The robot consists of a head attached to an endoscope, three grip units, two contraction units, and seven joints connecting the units: pneumatic tubes for driving these units, a tension spring, and a wire for the endoscope to inspect the pipe visually through the robot. Spring-fixing parts were attached to each end of the tension spring, as shown in Fig. 4(a).

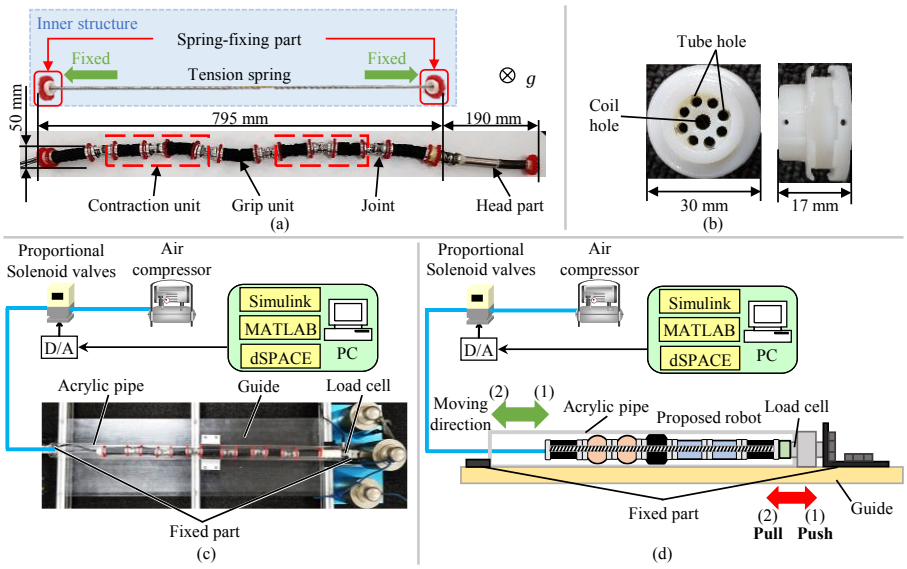

Fig. 4. Designed mechanism and experimental environment for measuring propulsion and traction. (a) Appearance of the developed robot. (b) Appearance of the spring-fixing part. (c) Actual experimental environment. (d) Experimental environment for measuring propulsion and traction.

B. *Tension Spring*

A tension spring was passed inside the robot, as shown in Fig. 4(a). This paper defines the tension spring as an endoskeleton. The tension spring behaves as a rigid body in the axial direction, making contraction challenging. By contrast, when subjected to a tensile load, extension occurred according to Hooke's law. These characteristics enable the transmission of the pushing force in the axial direction and bent in the Yaw and Pitch directions relative to the travel direction. In addition, the tension spring protects the passing endoscope wiring that passes inside the robot. In this study, a highly flexible tension spring with a spring constant of 0.0868 N/mm, a wire diameter of 0.9 mm, and an outer diameter of 0.6 mm was applied for testing purposes. To translate the contraction force of the actuator into propulsion and traction, the natural length of the tension spring was determined as the total length of the robot when one of the contraction units was contracted. Hence, the total length of the tension spring was set at 795 mm, corresponding to the total robot length during operation, as shown in Fig. 2 (iii).

C. *Spring-Fixing Part*

Fig. 4(b) shows the spring-fixing part. The spring-fixing part, created using a three-dimensional printer, had a central coil hole to fix the tension spring and eight outer holes for the air tubes. Both ends of the tension spring were fixed to the coil holes in the spring-fixing parts.

IV. Propulsion and Traction Measurement Experiment

This section describes the purpose, environment, methods, results, and discussion of the robot propulsion and traction measurements.

A. *Purpose*

The propulsion and traction of an in-pipe inspection robot equipped with a linear antagonistic mechanism using artificial endoskeletal muscles were measured. The differences in propulsion between the robots with and without the endoskeleton were compared.

B. *Environment and Method*

The measurement of propulsion and traction was conducted following the same method as in a previous study [19]. Fig. 4(c) shows the actual experimental environment, and Fig. 4(d) shows the experimental environment for the propulsion and traction measurement tests. Compressed air was supplied from a compressor via solenoid valves, and the robot was driven within an acrylic pipe with an inner diameter of 52 mm. For the propulsion measurement, the robot was connected to a load cell fixed to one side of the acrylic pipe. Thereafter, the robot in the pipe was propelled in the compression direction of the load cell for 120 s, as shown in Fig. 4(d) (1), and the pushing force was measured as the propulsion. In the traction measurement, the robot moved in the opposite direction to that in the propulsion measurement. The robot in the pipe was moved forward in the pulling direction of the load cell for 120 s, as shown in Fig. 4(d) (2), and the tensile force was measured as traction. The sampling frequency was 2 kHz and 0.15 MPa was applied to each unit, representing the minimum pressure required for the grip unit to expand beyond the inner diameter of the pipe and grip the pipe. The operation patterns and operation times shown in Fig. 2 were applied to the in-pipe inspection robot. The aim of this study was to demonstrate the effectiveness of the proposed mechanism using a basic robot operation pattern. Therefore, the effect of the robot-generated force with and without the endoskeleton was experimentally verified using the pure robot movement method. The propulsions exerted by the robot with and without the proposed mechanism were compared.

C. *Result*

The propulsion and traction when 0.15 MPa is applied to each unit are described. Fig. 5(a) shows the time series data of the robot propulsion without the linear antagonistic mechanism of the artificial muscles with an endoskeletal structure. Fig. 5(b) and 5(c) show the time series data of the robot's propulsion and traction with a linear antagonistic mechanism using artificial muscles with an endoskeletal structure. Fig. 5(d) shows a graph of the maximum propulsion with and without the endoskeleton of the robot.

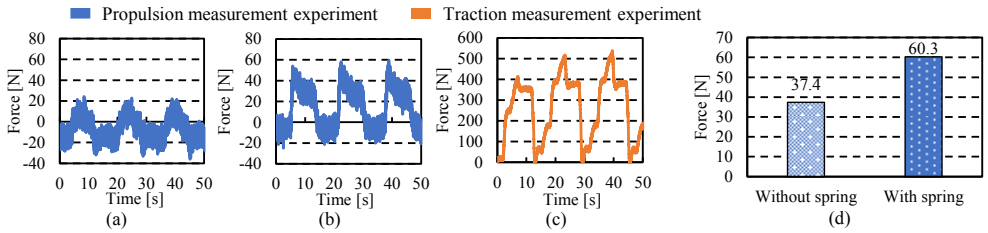

Fig. 5. Time series pipe inspection of the propulsion and traction of the robot. The propulsion and traction data applied to the robot at 0.15 MPa with the linear antagonistic mechanism using artificial muscles with an endoskeletal structure are described. (a) Propulsion (without the linear antagonistic mechanism using artificial muscles with an endoskeletal structure). (b) Propulsion (with the linear antagonistic mechanism using artificial muscles with an endoskeletal structure). (c) Traction (with the linear antagonistic mechanism using artificial muscles with an endoskeletal structure). (d) Comparison of maximum propulsion of robots with and without an endoskeleton.

D. Discussion

Figs. 5(a), 5(b), and 5(c) show that the same waveform trend was continuous in propulsion and traction because the robot repeated a constant operation. These forces increased from the beginning of the vibrating movement until the play was removed. The waveforms show that the force generated by the mechanism reached its maximum value during operation, as shown in Fig. 2(iv), becoming propulsive. Therefore, we believe that propulsion and traction were actively generated.

The propulsion exerted by the robot was increased by using an endoskeleton. Fig. 5(d) shows that when 0.15 MPa was applied to each unit, the maximum propulsion was 37.4 N for the robot without the linear antagonistic mechanism using artificial muscles with an endoskeletal structure and 1.61 times the maximum propulsion of 60.3 N for the robot with the linear antagonistic mechanism using artificial muscles with an endoskeletal structure. The maximum traction was 538.9 N for the robot with an endoskeleton. The maximum theoretical propulsion and traction for the linear antagonistic mechanism using artificial muscles with an endoskeletal structure were 42 and 544 N, respectively, when 0.15 MPa was applied to each unit. We considered the traction valid based on the basic characteristics of the contraction unit (Fig. 3(j)). However, there is a difference between the theoretical and measured propulsion values. This phenomenon is attributed to the addition of the pushing force by the tension spring, which results in the measured value being larger than the theoretical value. Therefore, we considered the measured value to be larger than the theoretical value because, in Fig.3(iv) operation, the endoskeleton not only transmitted the contraction force of the contraction unit but also exerted pushing force. In future, we will develop a theoretical model that considers spring force.

V. Elbow Pipe Passage Experiment

This section describes the verification results of the driving test with and without the linear antagonistic mechanism using artificial muscles with an endoskeletal structure for the in-pipe inspection robot to pass through a bent pipe.

A. Purpose

The movement performance of the in-pipe inspection robot was verified using simulated pipes with a single elbow pipe in a passage. The passage times of robots with and without endoskeletons were compared.

B. Environment and Method

Fig. 6(a) shows the experimental environment and Fig. 6(b) shows the actual simulated piping configuration. These pipes consisted of two clear acrylic straight pipes (1 m) placed horizontally on the ground, with one short elbow pipe. A linear antagonistic mechanism using artificial muscles with an endoskeletal structure was developed to provide propulsion and increase speed when loads such as bent pipes are generated. Therefore, the robot was started at point A, where the head passed through the elbow pipe, to observe the performance of the proposed mechanism when passing through a bent pipe. Subsequently, three inspections were conducted until the head passed through point C. A video camera captured the movement of the robot, and the passage of time was measured from the video images. The passage time of each unit to point B, the point after passing through the elbow pipe, was also measured. The average passage time of a bent pipe was calculated and compared with the average passage times of robots with and without the endoskeleton. The operation times shown in Fig. 2 were applied to the robot.

C. Result

The test results are presented in Fig. 6(c). The robot passed through the simulated pipes three times consecutively, with and without an endoskeleton. The average passage time to Point C for the robot without an endoskeleton was 741 s, whereas that for the robot with an endoskeleton was 574 s.

D. Discussion

The introduction of the endoskeleton into the robot reduced the average passage time of the bent pipe by approximately 22.3%. The proposed mechanism exhibited similar passage times for the three tests, indicating the high reproducibility of the experiment.

Comparing the average passage time of each unit to point B, as shown in Fig. 6(c), the proposed robot with the endoskeleton requires less time. Figs. 7(a) and 7(b) show the states of Figs. 2 (iii) and 2 (iv), respectively, when the proposed mechanism is subjected to loads from the propulsive and tractive directions while passing through a bending pipe. Owing to the force exerted on the tension spring, which does not contract in the axial direction, the proposed mechanism passes along the path depicted in Fig. 2 (iii). Subsequently, the active contraction force of the contraction unit is transmitted by the tension spring to exert propulsion, as shown in Fig. 2 (iv). We believed that the robot could pass through the bent pipe because the proposed mechanism exerted more

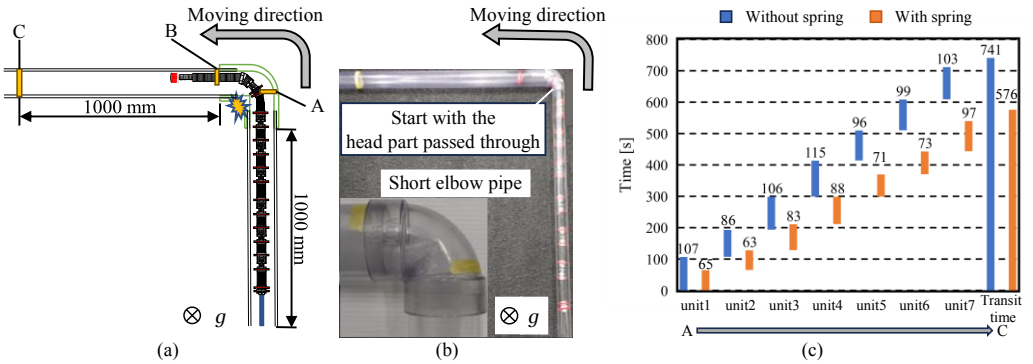

Fig. 6. (a) Experimental environment for measuring the transit time through a curved pipe. (b) Actual experimental environment. (c) Experimental results of passage through an elbow pipe with and without the linear antagonistic mechanism using artificial muscles with an endoskeletal structure.

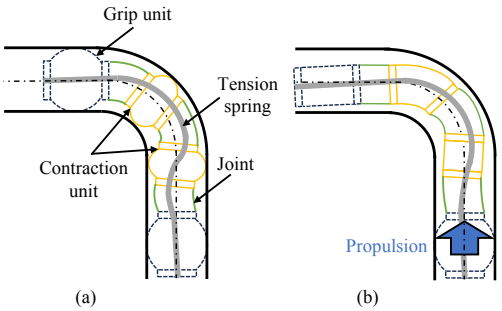

Fig. 7. Path model of a developed pipe inspection robot when passing through an elbow pipe. (a) The travel path of (iii), as shown in Fig. 2. (b)The travel path of (iv), as shown in Fig. 2.

propulsion than the load generated when the robot passed through the bent pipe.

VI. Comparison of Evaluation Functions

In this section, we present a numerical comparison of the propulsion and traction of the developed robot with those of the other inspection robots [22-29]. We evaluated propulsion and traction based on the evaluation function of a previous study [19]. This evaluation function is dimensionless and comparable to the mechanically available force even when the scale and applied pressure of the robot are different. The evaluation functions are expressed in (3), (4), and (5). Equations (3) and (4) express the nondimensionalized propulsion F_{DP} and traction F_{DT}, respectively. Equation (5) is the sum of (3) and (4), representing the evaluation function H_{EI} from a previous study.

The H_{EI} values are shown in Fig. 8, demonstrating that the in-pipe inspection robot equipped with the linear antagonistic mechanism using artificial muscles with an endoskeletal structure exhibited a 1.13-fold increase compared to the PI-RO II reported in a previous study [29]. In comparison with other pipe inspection robots, the F_{DT} of this robot was more than 1.55 times higher. The F_{DP} of the robot was sufficiently large to pass through a bent pipe. From the obtained results, we can expect a linear antagonistic mechanism using artificial muscles with an endoskeletal structure to enable the inspection robot to inspect small-diameter complex pipes, as traction and propulsion are significantly increased. Although the propulsion was lower than that in the previous study, the robot could pass through the bent pipe, as shown in Fig. 7. Thus, it is expected that the robot, developed to generate force through

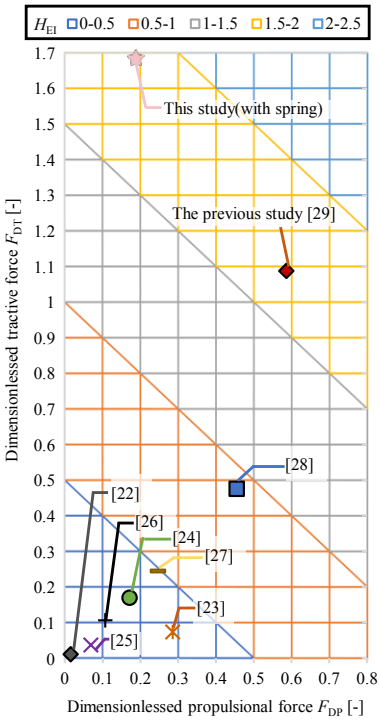

Fig. 8. Comparison of evaluation functions. The developed pipe-inspection robot exhibited a H_{EI} value 1.13 times higher than that of PI-RO II in the previous study [29].

$$F_{DP} = \frac{F_{Pro}}{A \cdot P} \tag{3}$$

$$F_{DT} = \frac{F_{Tra}}{A \cdot P} \tag{4}$$

$$H_{EI} = F_{DP} + F_{DT} \tag{5}$$

air pressure, will enable inspection of long, narrow, and complex pipes.

This study established a method for converting the muscle contraction force into the extension force and demonstrated the possibility of applying these biological advantages in robotics. The obtained results demonstrate the possibility of developing a new robot that uses the operating principles of earthworms. Furthermore, deliberately adding an endoskeleton to a naturally nonskeletal worm represents the development of a novel robotic mechanism that enhances biological functionality. This approach is expected to become applicable in the future.

VII. CONCLUSION

This study proposed a linear antagonistic mechanism using artificial muscles by inserting a tension spring (skeleton) inside contraction actuators to increase propulsion and traction enable the inspection of long, narrow, and complex pipes. The robot developed in this study exerted a maximum propulsion of 60.3 N and a maximum traction of 538.9 N. The propulsion was 1.61 times higher than that of the robot without the endoskeleton while exerting significant traction. The evaluation function value considering the effects of the applied pressure and inner diameter of the target pipe of the robot developed in this study was 1.13 times compared to that reported in a previous study. The nondimensionalized traction was more than 1.55 times higher than that of any other pipe inspection robot, and the propulsion was sufficiently large to pass through the pipes. Furthermore, the developed robot with the endoskeleton passed through the elbow pipe 1.29 times faster than that without the endoskeleton, reducing the time from 741 to 576 s. These results indicate that the proposed mechanism can enable robots to inspect narrow and complex pipes over long distances.

In future, we plan to verify the long-distance inspection performance of the developed robot using real factory pipes. We optimize wave locomotion to analyze energy consumption and test the robot's performance with varying pipe diameters and traction loads.

REFERENCES

[1] H. Masuta, H. Watanabe, K. Sato, H. Lim, "Recognition of Branch Pipe for Pipe Inspection Robot using Fiber Grating Vision Sensor," *In Proc. of The 2013 Int. Conf. on Ubiquitous Robots and Ambient Intelligence(URAI)*, Korea, Jeju, pp.633-638, Oct. 2013.

[2] S. Yoda, Y. Wakibe, Y Imagawa, "Inspection methods of piping," Bull. *Soc. Sea Water Sci.*, vol. 68, no. 2, pp. 57-62, Sep. 2014. (in Japanese)

[3] Q. Ma, G. Tian, Y. Zeng, R. Li, H. Song, Z. Wang, B. Gao and K. Zeng, "Pipeline In-Line Inspection Method, Instrumentation and Data Management," *Sensors 2021,* vol.21, no.11, Jun. 2021.

[4] M. A. A. Wahed, M. R. Arshad, "Wall-press type pipe inspection robot," In *Proc. of 2017 IEEE 2nd Int. Conf. on Automatic Control and Intell. Syst. (I2CACIS)*, Kota Kinabalu, Sabah, Malaysia, pp.185-190, Oct. 2017.

[5] B. Zhang, M. Abdulaziz, K. Mikoshi and H. Lim, "Development of an In-pipe Mobile Robot for Inspecting Clefts of Pipes," In *Proc. of 2019 IEEE Int. Conf. Cybernetics Intell. Syst. (CIS)* and *IEEE Conf. Robotics, Automation and Mechatronics (RAM)*, Bangkok, Thailand, pp.204-208, Nov. 2019.

[6] H. M. Kim, Y. S. Choi, Y. G. Lee, H. R. Choi, "Novel Mechanism for In-Pipe Robot Based on a Multiaxial Differential Gear Mechanism," *IEEE/ASME Trans. on Mechatronics*, Vol.22, No.1, pp.227-235, Oct. 2016.

[7] A. Kakogawa, S. Ma, "A Multi-link In-pipe Inspection Robot Composed of Active and Passive Compliant Joints," In *Proc. of 2020 IEEE/RSJ Int. Conf. on Intell. Robots Syst. (IROS)*, Las Vegas, NV, USA, pp.6472-6478, Oct. 2020.

[8] A. Kakogawa, S. Ma, "Design of an underactuated parallelogram crawler module for an in-pipe robot," *In Proc. of 2013 IEEE Int. Conf. on Robotics and Biomimetics (ROBIO)*, Shenzhen, China, pp.1324- 1329, Dec. 2013.

[9] S. Xiao, Z. Bing, K. Huang, Y. Huang, "Snake-like robot climbs inside different pipes," In *Proc. of 2017 IEEE Int. Conf. on Robotics and Biomimetics (ROBIO)*, Macau, Macao, Dec. 2017.

[10] A. Selvarajan, A. Kumar, D. Sethu, M. A. B. Ramlan, "Design and Development of a Snake-Robot for Pipeline Inspection," In *Proc. of 2019 IEEE Student Conf. on Research and Development (SCOReD)*, Bandar Seri Iskandar, Malaysia, pp.237-242, Oct. 2019.

[11] A. Zagler, F. Pfeiffer, ""MORITZ" a pipe crawler for tube junctions," In *Proc. of 2003 IEEE Int. Conf. on Robotics and Automation*, Taipei, Taiwan, pp.2954-2959, Sep. 2003.

[12] M. Rashid, F. Yakub, S. Zaki, M. Ali, N. Mamat, S. M. Putra, S. Roslan, H. Shah, M. Aras, M. Arshad, "Reconfigurable multi-legs robot for pipe inspection: Design and gait movement," *Indian J. of Geo Marine Sciences*, vol.48, no.7, pp.1132-1144, Jul. 2019.

[13] M. Konyo, K. Hatazaki, K. Isaki, S. Tadokoro "Development of an Active Scope Camera Driven by Cilia Vibration Mechanism," In *Proc. of 2006 IEEE/RSJ Int. Conf. on Intell. Robots Syst. (IROS)*, Beijing, China, pp.3946-3951, Oct. 2006.

[14] Y. Mano, R. Ishikawa, Y. Yamada, T. Nakamura, "Development of High-speed Type Peristaltic Crawling Robot for Long-distance and Complex-line Sewer Pipe Inspection," In *Proc. of 2018 IEEE/RSJ Int. Conf. on Intell. Robots Syst. (IROS)*, Madrid, Spain, pp.8177-8183, Oct. 2018.

[15] F. Ito, T. Kawaguchi, M. Kamata, Y. Yamada, T. Nakamura, "Proposal of a Peristaltic Motion Type Duct Cleaning Robot for Traveling in a Flexible Pipe", In *Proc. of 2018 IEEE/RSJ Int. Conf. Intell. Robots Syst. (IROS)*, China, Macau, pp.6614-6621, Nov. 2019.

[16] J. Min, Y. D. Setiawan, P. S. Pratama, S. B. Kim, H. K. Kim, ''Development and controller design of wheeled-type pipe inspection robot,'' In *Proc. of 2014 Int. Conf. Adv. Comput., Commun. Informat. (ICACCI)*, New Delhi, India, pp.789–795, Sep. 2014.

[17] S. A. Fjerdingen, P. Liljeback, and A. A. Transeth, ''A snake-like robot for internal inspection of complex pipe structures (PIKo),'' In *Proc. of 2019 IEEE/RSJ Int. Conf. Intell. Robots Syst. (IROS)*, St. Louis, MO, USA, pp.5665–5671, Oct. 2009.

[18] A. Hadi, M. Abdollahi, K. Alipour, and B. Tarvirdizadeh, ''Design and prototyping a new add-on module to increase traction force of a wheeled sewer inspection robot,'' In *Proc. of 2017 5th RSI Int. Conf. Robot. Mechatronics (ICRoM)*, Tehran, Iran, pp.254–259, Oct. 2017.

[19] F. Ito, K. Takaya, M. Kamata, M. Okui, Y. Yamada, T. Nakamura, "In-Pipe Inspection Robot Capable of Actively Exerting Propulsive and Tractive Forces with Linear Antagonistic Mechanism," *IEEE Access*, vol. 9, pp.131245-131259, Sep. 2021.

[20] R. Okuma, Y. Naruse, F. Ito, and T. Nakamura, "Proposal of a Moving Speed Enhancing Method for Peristaltic Motion Type In-Pipe Inspection Robot with Linear Antagonistic Mechanism Using Endoskeletal Type Artificial Muscles," In *Proc. of 2023 IEEE Int. Conf. on Robotics and Biomimetics (ROBIO)*, Koh Samui, Thailand, pp.1-6, Dec. 2023.

[21] T. Nakamura, "Experimental Comparisons between McKibben type Artificial Muscles and Straight Fibers Type Artificial Muscles," In *Proc. of SPIE Int. Conf. on Smart Structures, Devices and Systems III*, Adelaide, Australia, 641426, Jan. 2007.

[22] T. Yamamoto, M. Konyo, and S. Tadokoro, "A high-speed locomotion mechanism using pneumatic hollow-shaft actuators for in-pipe robots," In *Proc. of IEEE/RSJ Int. Conf. Intell. Robots Syst. (IROS)*, Hamburg, Germany, pp.4724-4730, Sep. 2015.

[23] J. Qiao, J. Shang and A. Goldenberg, "Development of inchworm in-pipe robot based on self-locking mechanism," *IEEE/ASME Trans. Mechatronics*, vol. 18, no. 2, pp.799-806, Apr. 2013.

[24] M. Kamata, S. Yamazaki, Y. Tanise, Y. Yamada and T. Nakamura, "Morphological change in peristaltic crawling motion of a narrow pipe inspection robot inspired by earthworm's locomotion," *Adv. Robot.*, vol.32, no.7, pp.386-397, Jan. 2018.

[25] H. Heung, P. W. Y. Chiu and Z. Li, "Design and prototyping of a soft earthworm-like robot targeted for GI tract inspection," In *Proc. IEEE Int. Conf. Robot. Biomimetics (ROBIO)*, Qingdao, China, pp.497-502, Dec. 2016.

[26] B. Zhang, Y. Fan, P. Yang, T. Cao and H. Liao, "Worm-like soft robot for complicated tubular environments," *Soft Robot.*, vol.6, no.3, pp.399-413, Jun. 2019.

[27] S. Kodama, Y. Konishi, K. Shindo, S. Senzaki, T. Nakamura, Y. Ohnuki, M. Konno, H. Isii and A. Takanishi, "Development of pneumatic driven robot system which can entry and retire from gas pipe," In *Proc. IEEE Int. Conf. Mechatronics Autom. (ICMA)*, Takamatsu, Japan, pp.1466-1471, Aug. 2021.

[28] F. Ito, K. Takaya, H. Sato, J. Watanabe, and T. Nakamura, "Wave propagation type pipe inspection robot with the linear antagonistic mechanism for enhancing traction force — Increasing tractive force with a small number of drive units using superposition of linear antagonistic mechanisms," *J. Robot. Soc. Jpn.*, vol.39, no.7, pp.665-668, 2021.

[29] F. Ito, Y. Naruse, K. Takaya, J. Watanabe, and T. Nakamura, "Traction amplified actuation system for inspecting narrow and complex pipes using enhanced linear antagonistic mechanism - Bend pipe passage model and force comparison," *IEEE Access*, vol.11, Jul. 2023.